Sleep Medicine 115 (2024) 5–13

Contents lists available at ScienceDirect

Sleep Medicine

journal homepage: www.elsevier.com/locate/sleep

Functional connectivity-based classification of rapid eye movement sleep behavior disorder

Toma Matsushima [a,b], Kenji Yoshinaga [c], Noritaka Wakasugi [a], Hiroki Togo [a,c], Takashi Hanakawa [a,c,*], Japan Parkinson's Progression Markers Initiative (J-PPMI) study group[1]

[a] Department of Advanced Neuroimaging, Integrative Brain Imaging Center, National Center of Neurology and Psychiatry, Kodaira, Tokyo, 187-8501, Japan
[b] Department of Biotechnology and Life Science, Tokyo University of Agriculture and Technology, Koganei, Tokyo, 184-8588, Japan
[c] Department of Integrated Neuroanatomy and Neuroimaging, Kyoto University Graduate School of Medicine, Kyoto, 606-8501, Japan

ARTICLE INFO

Keywords:
Resting-state functional magnetic resonance imaging
Functional connectivity
Rapid eye movement sleep behavior disorder
Machine learning

ABSTRACT

Background: Isolated rapid eye movement sleep behavior disorder (iRBD) is a clinically important parasomnia syndrome preceding α-synucleinopathies, thereby prompting us to develop methods for evaluating latent brain states in iRBD. Resting-state functional magnetic resonance imaging combined with a machine learning-based classification technology may help us achieve this purpose.
Methods: We developed a machine learning-based classifier using functional connectivity to classify 55 patients with iRBD and 97 healthy elderly controls (HC). Selecting 55 HCs randomly from the HC dataset 100 times, we conducted a classification of iRBD and HC for each sampling, using functional connectivity. Random forest ranked the importance of functional connectivity, which was subsequently used for classification with logistic regression and a support vector machine. We also conducted correlation analysis of the selected functional connectivity with subclinical variations in motor and non-motor functions in the iRBDs.
Results: Mean classification performance using logistic regression was 0.649 for accuracy, 0.659 for precision, 0.662 for recall, 0.645 for f1 score, and 0.707 for the area under the receiver operating characteristic curve ($p < 0.001$ for all). The result was similar in the support vector machine. The classifier used functional connectivity information from nine connectivities across the motor and somatosensory areas, parietal cortex, temporal cortex, thalamus, and cerebellum. Inter-individual variations in functional connectivity were correlated with the subclinical motor and non-motor symptoms of iRBD patients.
Conclusions: Machine learning-based classifiers using functional connectivity may be useful to evaluate latent brain states in iRBD.

* Corresponding author. Department of Integrated Neuroanatomy and Neuroimaging, Kyoto University Graduate School of Medicine, Yoshida-Konoe, Sakyo-ku, Kyoto, 606-8501, Japan.
E-mail address: hanakawa.takashi.2s@kyoto-u.ac.jp (T. Hanakawa).

[1] Noriko Nishikawa[a,e], Miho Murata[a†], Taku Hatano[e], Yohei Mukai[a], Yuji Saitoh[a], Takashi Sakamoto[a], Takashi Hanakawa[b], Yuichi Kamei[c,q], Hisateru Tachimori[d], Kenji Hatano[d], Hiroshi Matsuda[b], Yosuke Taruno[g], Nobukatsu Sawamoto[g], Yuta Kajiyama[h], Kensuke Ikenaka[h], Kazuya Kawabata[i,k], Tomohiko Nakamura[k,l], Hirotaka Iwaki[p], Hiroshi Kadotani[r], Yukiyoshi Sumi[r], Yuichi Inoue[s,t], Toshihiro Hayashi[m,n], Takeshi Ikeuchi[o], Yasushi Shimo[e,f], Hideki Mochizuki[h], Hirohisa Watanabe[i,j], Nobutaka Hattori[e], Yuji Takahashi[a], Ryosuke Takahashi[g]: a. Department of Neurology, National Center Hospital, National Center of Neurology and Psychiatry (NCNP), b. Integrative Brain Imaging Center, NCNP, c. Department of Sleep-Wake Disorder, National Institute of Mental Health, NCNP, d. Department of Clinical Data Science, Clinical Research and Education Promotion Division, NCNP, e. Department of Neurology, Juntendo University Graduate School of Medicine, f. Department of Neurology, Juntendo Nerima Hospital, g. Department of Neurology, Kyoto University Graduate School of Medicine, h. Department of Neurology, Osaka University Graduate School of Medicine, i. Brain and Mind Research Center, Nagoya University Graduate School of Medicine, j. Department of Neurology, School of Medicine, Fujita Health Univesity, k. Department of Neurology, Nagoya University Graduate School of Medicine, l. Department of Neurology, Hamamatsu University School of Medicine, m. Department of Neurology, The University of Tokyo Graduate School of Medicine, n. Department of Physiology, Teikyo University School of Medicine, o Department of Molecular Genetics, Brain Research Institute Niigata University, p. Data Tecnica International, q. Department of Psychiatry, Kamisuwa Hospital, r. Department of Psychiatry, Shiga University of Medical Science, s. Japan Somnology Center, Neuropsychiatric Research Institute, t. Department pf Somnology, Tokyo Medical University.

https://doi.org/10.1016/j.sleep.2024.01.019
Received 23 April 2023; Received in revised form 13 January 2024; Accepted 16 January 2024
Available online 22 January 2024

1. Introduction

Abbreviations

REM	rapid eye movement
RBD	REM sleep behavior disorder
iRBD	isolated RBD
PD	Parkinson's disease
DLB	dementia with Lewy bodies
MSA	multiple system atrophy
MRI	magnetic resonance imaging
fMRI	functional MRI
rsfMRI	resting-state fMRI
FC	functional connectivity
ML	machine learning
J-PPMI	Japan-Parkinson's Disease Progressive Markers Initiative
SVM	support vector machine
HC	healthy control
NCNP	National Center of Neurology and Psychiatry
RBDSQ-J	Japanese edition of the RBD screening questionnaire
ESS	Epworth Sleepiness Scale
MDS-UPDRS	Movement Disorder Society-sponsored revision of the Unified Parkinson's Disease Rating Scale
MoCA-J	Japanese version of the Montreal Cognitive Assessment
TR	repetition time
TE	echo time
FA	flip angle
ICA	independent component analysis
cAIC	corrected Akaike's information criteria
AUC	area under the receiver operating characteristic curve
TP	true positive
TN	true negative
FP	false positive
FN	false negative

Rapid eye movement (REM) sleep behavior disorder (RBD) is a parasomnia characterized by dream enactment behavior and REM sleep without atonia. RBD may be diagnosed alone as isolated RBD (iRBD). RBD is defined secondary when it co-exists with Parkinson's disease (PD) and related disorders. iRBD may accompany mood symptoms, cognitive impairment, and autonomic dysfunctions, and, moreover, may prelude α-synucleinopathies including PD. Indeed, over 70 % of patients with iRBD develop PD, dementia with Lewy bodies (DLB), or multiple system atrophy (MSA) within 12 years [1], all of which are α-synucleinopathies from the perspective of molecular pathology. Therefore, in older adults, the early diagnosis of iRBD roughly equates to that of prodromal α-synucleinopathies [2,3], opening opportunities to develop early interventions. Currently, a diagnosis of iRBD is made with overnight polysomnography (PSG). Although PSG provides rich electroencephalographic information about cortical dynamics and autonomic nervous system, more information is needed for studying prodromal α-synucleinopathies involving the subcortical regions such as the basal ganglia and cerebellum. Thus, methodological development is needed to evaluate latent functional changes of the brain in iRBD as α-synucleinopathy.

Magnetic resonance imaging (MRI) is used widely as a tool for medical diagnosis and evaluation including the exclusion of RBD following organic lesions in the brainstem (e.g. Ref. [4]). Although currently available structural MRI contrasts cannot differentiate iRBD from other medical conditions without organic lesions, functional MRI (fMRI) may help us retrieve information about latent brain functions in patients with iRBD. Many fMRI studies have already been conducted in patients with RBD, using a task [5] or resting-state fMRI (rsfMRI) [6–8]. Most rsfMRI studies analyzed functional connectivity (FC), which represents the correlation of spontaneous rsfMRI signal fluctuations between remote brain regions [9]. Those rsfMRI studies have suggested that FC contains information that characterizes the network abnormalities of iRBD.

Given the possibility of retrieving useful information from FC, building a classifier to identify individuals with iRBD according to FC may be plausible. Herein, a classifier refers to software that can learn from previous data to adequately weight a set of FC values relevant to differentiating between people with and without iRBD. The classifier can determine whether an individual should be labeled as iRBD when it is provided with rsfMRI-derived FC information. Notably, however, the number of FC values amounts to ~8500 when computed from a set of volumes of interest, e.g., the Automated Anatomical Labeling system [10]. Therefore, to select and compute adequate weights on relevant FC values, machine learning (ML) technology with an adequate dimension reduction method is required.

Here we aimed to develop an FC-based ML classifier of people with iRBD, using single-site data registered in the Japan-Parkinson's Disease Progressive Markers Initiative (J-PPMI) cohort [11]. We used a random forest for dimensionality reduction and feature selection, and a support vector machine (SVM) or a logistic regression for supervised classification. First, we hypothesized that the FC-based ML classifier would be able to differentiate between iRBD patients and healthy controls (HCs), by selecting a set of FC value changes associated with latent α-synucleinopathies. This was a hypothesis-free process about the specific FCs. Second, we hypothesized that the FC values selected by the ML classifier would correlate with the subclinical motor symptoms and cognitive alterations of patients with iRBD. Such FC should involve the primary and higher motor areas, somatosensory areas, basal ganglia, thalamus, and cerebellum as previously reported in FC studies in iRBD [6–8]. If such FCs can be retrieved from rsfMRI by ML, then the utility of ML-based rsfMRI may be suggested as a method to evaluate latent functional changes underlying subclinical symptoms of prodromal α-synucleinopathies.

2. Methods

2.1. Participants

Fifty-five patients with iRBD (aged 69.6 ± 5.8 years; age range 60–83 years; 39 men) were recruited at the National Center of Neurology and Psychiatry (NCNP) site of the J-PPMI cohort (Table 1). The inclusion and exclusion criteria of the J-PPMI cohort were described previously [11]. In brief, the J-PPMI cohort recruited patients with iRBD. The diagnosis of iRBD was made by sleep specialists according to the International Classification of Sleep Disorders criteria, 3rd revision. Overnight PSG with electromyography over the chin and tibialis anterior muscles confirmed REM sleep without atonia in accordance with the American Academy of Sleep Medicine criteria 2007 [12]. Co-existence of PD/DLB, MSA, dementia, and severe depression was excluded by expert physicians at the NCNP. All iRBD participants provided written informed consent, and the study protocol was approved by the NCNP ethics committee (A2014-127).

To serve as a control, we retrieved data from our MRI database approved by the NCNP ethics committee (A2018-056) [7,13]. The original inclusion criterion of this database was healthy adults aged >20 years old without any previous history of neuro-psychiatric disorders.

Table 1
Profile of study participants.

	RBD (N = 55)	HC (N = 97)	statistics
Demographic Data			
Age (years)	69.6 ± 5.8	66.3 ± 8.7	$t = 2.56$, $p < 0.01$
Sex (Male/Female)	39/16	47/50	$\chi^2 = 7.24$, $p < 0.007$
Clinical and neuropsychological assessment			
RBDSQ-J	7.6 ± 2.9	NA	
ESS	5.2 ± 3.1	NA	
MDS-UPDRS I	4.6 ± 3.4	NA	
MDS-UPDRS III	1.7 ± 1.9	NA	
MMSE	28.5 ± 1.3*	28.9 ± 1.1	F = 1.16, p = 0.28 by ANCOVA
MoCA-J	24.9 ± 2.9	NA	
GDS	2.0 ± 2.0	NA	

Data shown are the mean ± SD. RBD, rapid eye movement sleep behavior disorder; HC, healthy control; SD, standard deviation; RBDSQ-J, Japanese edition of RBD screening questionnaire; ESS, Epworth Sleepiness Scale. MDS-UPDRS, Movement Disorder Society-sponsored revision of the Unified Parkinson's Disease Rating Scale; MMSE, mini-mental state examination; MoCA-J, Japanese version of Montreal Cognitive Assessment; GDS, Geriatric Depression Assessment; MoCA-J scores are adjusted for years of education; *converted from MoCA-J; NA, not available; For the comparison of MMSE, ANCOVA (analysis of covariance) was used to remove the effects of age.

None of the HCs had organic brain lesions as confirmed with structural MRIs. In all but one HCs, cognitive states were assessed using the mini-mental state examination (MMSE) to exclude dementia (exclusion criteria, MMSE<24). The HCs did not undergo PSG. For the present study, we retrieved data of 97 registered participants (aged 66.3 ± 8.7 years; age range 41–83 years; 47 men) from the database. Between the iRBD patients and HCs, there were group-wise differences in age ($t = 2.56$, $p < 0.01$) and sex ($\chi^2 = 7.24$, $p < 0.007$) (Table 1), which required caution while building the classifier.

Some of the data (50 iRBD patients and 70 HCs) have been used in our previous rsfMRI study in iRBD [7]. Among the 55 patients with iRBD, 35 patients received medication at the enrollment after PSG. Six patients received low-dose pramipexole (0.125–0.25 mg/day), 24 patients received clonazepam (0.125–2.5 mg/day), and two patients received ramelteon (4–8 mg/day). Two patients were taking both clonazepam and ramelteon, and one patient was taking all three medications.

2.2. Data acquisition

2.2.1. Clinical and neuropsychological assessments in iRBD

In the iRBD patients, RBD symptoms were screened at the enrollment by the Japanese edition of the RBD screening questionnaire (RBDSQ). Daytime sleepiness was assessed using the Epworth Sleepiness Scale (ESS). The Movement Disorder Society-sponsored revision of the Unified Parkinson's Disease Rating Scale (MDS-UPDRS) Part I and III scores were acquired by qualified movement disorder specialists. A higher score indicated more severe non-motor and motor symptoms associated with PD. Patients also completed the Japanese version of the Montreal Cognitive Assessment (MoCA) to assess cognitive functions and the Geriatric Depression Assessment to assess mood changes. In these scores except MoCA, higher scores indicate greater severity. The MoCA scores in iRBD were converted into MMSE scores [14] for statistical comparison between the groups.

2.2.2. MRI data acquisition

All participants were scanned on a 3-T MRI scanner with a 32-channel phased array head coil (MAGNETOM Verio Dot, Siemens Medical Systems, Erlangen, Germany). RsfMRI data were acquired using a gradient-echo echo planar imaging sequence for 10 min: repetition time (TR) = 2500 ms, echo time (TE) = 30 ms, flip angle (FA) = 80°, voxel size = 3.3 × 3.3 × 3.2 mm^3 (with a 0.8-mm inter-slice gap), 40 axial slices, and 240 volumes. During rsfMRI, participants were asked to stay awake, clear their minds, and pay attention to a central fixation cross presented on a screen. A double-echo gradient-echo sequence was used to acquire field-map MRI data in the same space and spatial resolution: TR = 488 ms, TE1 = 4.92 ms, TE2 = 7.38 ms, FA = 60°. Structural MRI data were acquired using a three-dimensional T1-weighted magnetization-prepared rapid gradient-echo sequence: TR = 1900 ms, TE = 2.52 ms, inversion time = 900 ms, FA = 90°, 192 sagittal slices, and voxel size = 0.98 × 0.98 × 1 mm^3.

2.3. Data analysis

2.3.1. Preprocessing of MRI data

For image preprocessing, we used the FMRIB Software Library [15] and CONN toolbox [16] implemented in MATLAB (MathWorks, Natick, MA, USA). We performed the following spatial and temporal preprocessing steps: realignment, distortion correction using field-map images, slice-time correction, spatial normalization, and smoothing with a full-width at half-maximum of 6 mm. The preprocessed rsfMRI data were denoised using Component-based Noise Correction [17], followed by further denoising using single-session independent component analysis (ICA) and FMRIB's manually-trained ICA-based Xnoiseifier.

After the intensive preprocessing, the whole brain was segmented into a set of 132 vol of interest based on the Automated Anatomical Labeling system. A set of FC values was computed for each participant as a correlation matrix, yielding a set of 8646 Pearson's correlation coefficients, which were subsequently converted into z-scores using Fisher's r-to-z transformation. To deal with the difference in age and sex between the groups, these z-scores were then corrected for the effects of age and sex, using general linear models (GLM). These corrected FC values are referred simply to as FC(s) hereafter.

2.3.2. Supervised ML algorithm

The original features were 8646 FCs from each of the 152 participants. To classify iRBD patients and HCs, we constructed an ML classification pipeline (Fig. 1), using *scikit-learn* version 1.1.1 and Python version 3.8.2. Briefly, we first dealt with the unbalanced sample size of the datasets between the iRBD patients (n = 55) and HCs (n = 97). We randomly selected 55 datasets out of the pool of 97 HC datasets and created HC subsamples iteratively 100 times. For each HC subsample, stratified 10-fold cross-validation was performed to yield balanced sample sizes between iRBD patients and HCs for both the training data and test data in each fold ($k = 10$). We did not perform hyperparameter tuning for the random forest or classification algorithms because unbiased hyperparameter tuning requires a larger dataset using another validation scheme (e.g., nested cross-validation).

2.3.3. Feature selection

We used the random forest (*RandomForestClassifier* in *scikit-learn*) for feature selection and sorting relevance of each FC for classification. The random forest sampled data with replacements from the training data to produce sub-datasets of the features. The decision trees were then constructed using each feature sub-dataset. Each decision tree randomly selected a feature from each sub-dataset, and the feature that minimized data variance was considered important. The importance of a feature was determined by the degree of data variance reduction due to the inclusion of the feature. The random forest used a majority vote from the decision trees for the final output. Five thousand initial decision trees were generated with a random state of 1. For each training dataset, we applied the random forest to compute the contribution of each FC to the classification of iRBD and HC labels, which provided a combination of each FC and its weight.

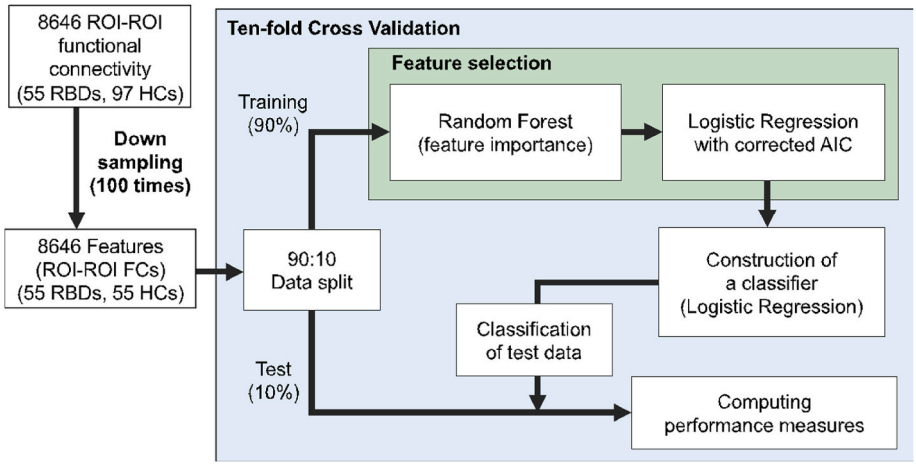

Fig. 1. The workflow of the classification. Classification was performed using 10-fold cross-validation for each down-sampling of HC datasets. The number of FC values was determined by the corrected Akaike information criteria (cAIC) for both logistic regression and support vector machine (SVM).

2.3.4. Dimensional reduction and classification

We conducted a logistic regression to classify iRBD patients and HCs, using FCs passed from the random forest module. Logistic regression (*scikit-learn*) was run, using a default regularization parameter of C = 1 and *liblinear* for parameter selection. To train the logistic regression model, we increased the number of features (FCs passed from the random forest) one at a time, starting with the feature with the highest weight. We then determined the final logistic regression model with the corrected Akaike's information criteria (cAIC) to select the model and reduce the dimension. Namely, we computed cAIC for each model and then selected the model with the minimum cAIC. This process effectively reduced the data dimension. We selected the final model for each fold to classify iRBD patients and HCs. The performance of the classification was evaluated as the average of the performance measures across the 10 folds for each of the 100 downsampling procedures.

For the validation of the classification results with logistic regression, we also conducted classification with a SVM (*scikit-learn*) using the following parameters: rbf (Gaussian kernel) with the default gamma value (1/[number of features × variance of the FCs]), the default regularization parameter of C = 1, and the 'probability = true' for computing the cAIC.

2.3.5. Evaluation of performance

To evaluate classification performance, we computed accuracy, precision, recall, f1, and the area under the receiver operating characteristic curve (AUC) using the number of true positives (TPs), true negatives (TNs), false positives (FPs), and false negatives (FNs) as follows:

$$\begin{aligned} accuracy &= \frac{TP+TN}{TP+TN+FP+FN} \\ precision &= \frac{TP}{TP+FP} \\ recall &= \frac{TP}{TP+FN} \\ f1 &= \frac{2\times precision\times recall}{precision+recall} \end{aligned} \quad (1)$$

2.3.6. Statistics

Age and sex were compared between iRBD and HCs, using a *t*-test and a chi-square test, respectively. MMSE was compared between the groups, with an analysis of covariance using age as a confounding factor.

We computed a surrogate marker for the distribution of classification performance. We shuffled the labels for iRBD and HC and ran the classification using the same pipeline 1000 times (10-fold cross-validation for each of the 100 downsampling procedures). T-tests were used to compare the classification performance (i.e., accuracy, precision, recall, f1, and AUC) between the truly labeled data and the randomly labeled data. We used $p < 0.05$ after Bonferroni correction for multiple comparisons for significance.

We counted the number of times the random forest selected each FC during the 1000 iterations. The repeatedly selected FCs were considered to contain clinically relevant information. We retrieved these frequently selected FCs and tested whether they differed between the iRBD patients and HCs using a *t*-test ($p < 0.05$ after Bonferroni correction for multiple comparisons).

Finally, we tested whether the selected FCs for the classification could correlate with the behavioral or clinical parameters (MDS-UPDRS Part I, MDS-UPDRS Part III, MoCA-J, ESS, and RBDSQ-J scores) in patients with iRBD. The effects of age and sex were regressed out from the original correlation coefficients from the iRBD individuals, using a dedicated GLM including age, sex, and each clinical parameter. We used stepwise regression with the FCs and the power of each FC as explanatory variables and did cAIC for model selection. An F-test was used to test the statistical inference of the stepwise regression after Bonferroni correction for multiple comparisons for the number of models tested.

3. Results

3.1. Clinical and neuropsychological assessments

The results from the clinical and neuropsychological assessments in iRBD were as follows (Table 1): RBDSQ-J = 7.6 ± 2.9, ESS = 5.2 ± 3.1, MDS-UPDRS part I = 4.6 ± 3.4, MDS-UPDRS part III = 1.7 ± 1.9, MoCA = 24.9 ± 2.9, GDS = 2.0 ± 2.0. These values were subsequently used for the correlation analysis with FCs.

In HCs, the MMSE scores were 28.9 ± 1.1 (n = 96), which were not different from the converted MMSE scores (28.5 ± 1.3) in iRBD (F = 1.16, p = 0.28 after the removal of age effects by analysis of covariance).

3.2. Classification performance

The logistic regression model yielded classification performance of ~65%–70 % consistently across the different performance measures: accuracy = 0.649 ± 0.004, precision = 0.659 ± 0.005, recall = 0.662 ± 0.006, f1 = 0.645 ± 0.005, and AUC = 0.707 ± 0.005 (Fig. 2). These performance measures were significant according to t-tests (Bonferroni corrected $p < 0.001$) as compared with the surrogate markers (i.e., classification performance with the disease label randomly shuffled). Classification performance of the SVM was comparable and also

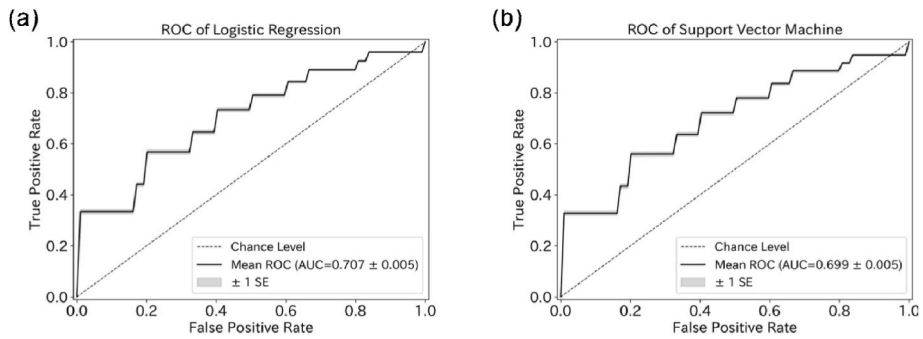

Fig. 2. (a) ROC for logistic regression yielded an AUC of 0.707 ± 0.005 (mean ± standard error). (b) The ROC for the SVM yielded an AUC of 0.699 ± 0.005.

significant (accuracy of 0.651 ± 0.004, precision of 0.659 ± 0.005, recall of 0.668 ± 0.006, f1 of 0.649 ± 0.005, and AUC of 0.699 ± 0.005; Bonferroni corrected $p < 0.001$). When we re-ran the classification between the iRBD patients and HCs >60 years (n = 83, age 68.9 ± 5.8 years), the performance was also comparable as follows: accuracy = 0.664 ± 0.004, precision = 0.671 ± 0.005, recall = 0.688 ± 0.006, f1 = 0.666 ± 0.005, and AUC = 0.723 ± 0.005. This analysis confirmed that after the removal of the effects with GLM, the performance was not likely affected by the group-wise difference in age.

3.3. Functional connectivity selected for classification

The median and interquartile range of the number of features (i.e., FCs) used for the classification were 9 and 7–11, respectively. Fig. 3 and Table 2 showed the nine most frequently used functional pathways, among which five positive and one negative FC values were significantly stronger in iRBD patients while two positive and one negative FCs were weaker. Most of these FCs involved the motor and somatosensory areas and the cerebellum. Five FCs were cortico-cerebellar connections, and one was intra-cerebellar connection. The anterior cingulate cortex, parahippocampal gyrus, anterior middle temporal gyrus and thalamus were also involved.

3.4. Correlation between functional connectivity and clinical and behavioral scores

In the stepwise multiple regression analysis, the FCs were correlated with MDS-UPDRS Part III ($F [2,18] = 5.326$, $p = 0.039$), and MoCA-J scores ($F [2,18] = 6.057$, $p = 0.022$), but not with MDS-UPDRS Part I, ESS or RBDSQ-J scores (Table 3). Sensorimotor-temporal, and sensorimotor-cerebellar FCs were correlated with the MDS-UPDRS Part III score. Sensorimotor-cerebellar and intra-cerebellar FCs were correlated with the MoCA-J score.

Table 2
Functional connectivity used for classification.

No.	FC		RBD (mean ± std)	HC (mean ± std)	p value
	ROI 1	ROI 2			
1	Lt. Postcentral Gyrus	Rt. Cerebellum 4/5	0.294 ± 0.172	0.120 ± 0.245	0.0001
2	Cingulate Gyrus anterior division	Rt. Thalamus	0.325 ± 0.200	0.192 ± 0.229	0.0044
3	Lt. Cerebellum 4/5	Vermis 8	0.247 ± 0.177	0.398 ± 0.209	0.0001
4	Lt. Precentral Gyrus	Rt. Cerebellum 6	0.309 ± 0.288	0.133 ± 0.210	0.0003
5	Lt. Precentral Gyrus	Rt. Cerebellum 4/5	0.331 ± 0.171	0.161 ± 0.230	0.0000
6	Rt. Supplementary Motor Area	Rt. posterior Parahippocampal Gyrus	0.053 ± 0.129	−0.047 ± 0.196	0.0091
7	Lt. Postcentral Gyrus	Cingulate Gyrus posterior division	0.030 ± 0.179	−0.108 ± 0.207	0.0006
8	Rt. Anterior Middle Temporal Gyrus	Rt. Cerebellum 9	0.129 ± 0.179	0.254 ± 0.197	0.0015
9	Lt. Postcentral Gyrus	Lt. Cerebellum 4/5	0.206 ± 0.200	0.058 ± 0.206	0.0003

Std, standard deviation; Lt, left; Rt, right.

4. Discussion

We developed ML-based technology to classify between patients with iRBD and HCs. To our knowledge, this is the first report to use ML and rsfMRI-derived FC for classifying iRBD patients. Recently, an increasing number of studies have applied ML-based classification to

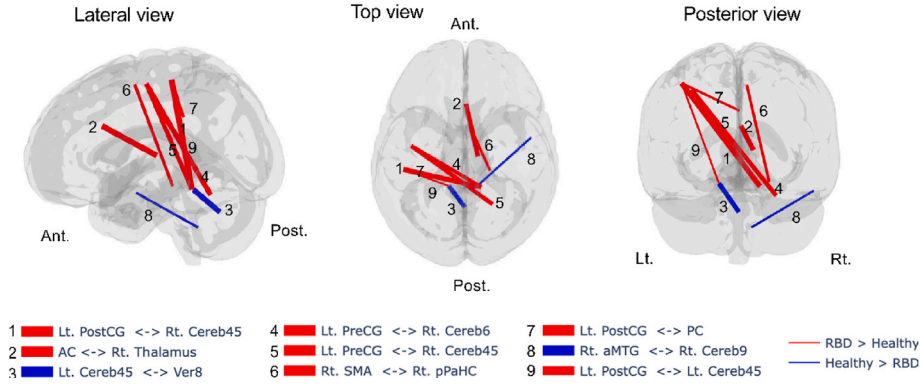

Fig. 3. (Color in print). The thickness of the lines represents the frequency of selection of the nine pathways. The red and blue lines indicate higher and lower FC, respectively, in iRBD patients relative to HCs. Refer to Table 3 for the nomenclature of FC. (For interpretation of the references to color in this figure legend, the reader is referred to the Web version of this article.)

Table 3
Functional pathways used in the stepwise regression.

FC		coefficient	std error	T value	p value
ROI 1	ROI 2				
MDS-UPDRS Part III					
Rt. Supplementary Motor Area	Rt. posterior Parahippocampal Gyrus	−0.716	0.266	−2.690	0.010
Lt. Precentral Gyrus[a]	Rt. Cerebellum 4/5[a]	0.727	0.266	2.734	0.009
MoCA					
Lt. Postcentral Gyrus	Rt. Cerebellum 4/5	−1.184	0.364	−3.250	0.002
Lt. Cerebellum 4/5	Vermis 8	0.529	0.364	1.451	0.153

Lt, left; Rt, right.
[a] Squared functional connectivity.

structural connectivity [19], gait parameters [20], and olfaction testing [21] to discriminate iRBD patients from HCs. This rise in ML research reflects the recent recognition of iRBD as a prodromal stage of α-synucleinopathies [22]. With a validation procedure, the classification performance of these previous studies substantially varies (sensitivity of 0.65–0.88 and specificity of 0.55–1.00) 19–21, depending on the features and ML methods. The classification performance of the present approach was statistically significant yet modest (sensitivity of 0.67–0.69 and specificity of 0.66–0.67). Notably, however, the selected FCs were correlated with clinical scores (MDS-UPDRS Part III and MoCA-J scores), supporting that the present ML method retrieved clinically relevant information from FCs. Although further research is needed to make the proposed method relevant to clinical practice, our findings suggest that ML-based analysis of rsfMRI data can retrieve latent functional changes in iRBD.

4.1. Classification technology combining machine learning and functional connectivity

Despite statistical significance against the surrogate marker, the performance of the classifier was modest. There are several possible reasons for this modest performance. First, our disease label was not perfectly precise because of the heterogeneity of individuals with iRBD who may develop different phenotypes of α-synucleinopathies in due course. Many previous studies reported that patients with iRBD are later phenoconverted to either PD, DLB or MSA [1,23–26] and alterations of FCs vary considerably among these diseases [27,28]. Although it is important to understand the differences between the phenotypes of α-synucleinopathy during the prodromal stage [29], differences in FC have not yet been determined. Additionally, the present iRBD patients should include various stages of prodromal α-synucleinopathies, which may be manifested soon or after a decade. To characterize FCs depending on the difference in the phenotypes and the prodromal stages, longitudinal studies of iRBD cohorts with the follow-up of outcomes are required. Indeed, the J-PPMI has followed up the present iRBD patients and will provide valuable data in the future to build a classifier that can take differences in the phenotypes and the prodromal stages into account. Second, although both iRBD patients and HCs were scanned using the same imaging protocol on the same MRI scanner, the rsfMRI data of HCs were obtained from our imaging database. It should be noted that the HCs did not undergo assessments such as PSG to exclude the presence of iRBD. Because iRBD is exhibited only during sleep, it often goes unrecognized unless the individual is explicitly questioned [30]. Therefore, we were unable to exclude the possibility that some of our HCs had iRBD. However, because the prevalence of iRBD in the general population is 0.4–1% [31,32], only one out of our 97 HCs might statistically have had unrecognized iRBD. Thus, the lack of screening PSG in HCs would not have strongly impacted the results.

Another reason for the modest performance of the classifier is that we considered the generalizability of the study inferences. We tried to minimize the use of noise in the rsfMRI data in the classification. RsfMRI data are notorious for the contamination of physical and physiological noise because of the low contrast-to-noise ratio. Nevertheless, numerous previous studies have shown high classification accuracy with a minimum amount of preprocessing. However, it has become apparent that ML classification may yield high classification performance by fitting to noise [33]. Therefore, we removed both spatial distortions and temporal noise from the rsfMRI data via rigorous preprocessing to minimize the risk of using noise information for the classification (e.g., one group had specific head motion patterns within the scanner). Moreover, we performed random downsampling of the HC data to obtain balanced training and test datasets between iRBD patients and HCs for cross-validation to reduce classifier bias. Indeed, a classifier classifying all participants as HCs can achieve high performance when using unbalanced datasets [33].

4.2. Interpretation of functional connectivity

In previous rsfMRI studies, iRBD patients were characterized by altered cortical FC in motor and somatosensory [7,8], prefrontal [7], visual [34], and parietal and temporal association networks [35]. Furthermore, the subcortical networks involving the basal ganglia [6,7,36,37] and cerebellum [8] have been shown to be distorted in iRBD.

To gain insight into these network abnormalities, we assessed the nine FCs that were most frequently selected by the classifier. In terms of the subcortical nodes, our classifier did not select FCs involving the basal ganglia, even though previous studies have reported FC abnormalities in the basal ganglia. The reason for this may be that less than half of our patients with iRBD showed a loss in dopamine terminals as measured by dopamine transporter scans [11].

Our classifier selected several FCs involving the cerebellum, which has been implicated in the pathogenesis of PD [38] following the discovery of the anatomical pathways connecting between the basal ganglia and the cerebellum. Of the cortico-cerebellar pathways in our results, four connected the primary somatosensory and motor areas with the cerebellum. Consistently, Yamada et al. [8] reported higher motor and somatosensory-cerebellar FC in iRBD patients with mild motor impairment than in those without. We also identified altered FC between the cerebellum and temporal cortex, which is compatible with the findings of a study in PD patients with RBD [39]. Although abnormal FC between cerebellar subregions has not previously been reported, our finding agrees with the report of abnormal regional homogeneity in the cerebellum [40]. However, whether abnormal cerebellar activity or connectivity in patients with PD or prodromal PD is pathogenic or compensatory remains unclear.

The FC between the right supplementary motor area and the right parahippocampal gyrus was stronger in iRBD. To our knowledge, an alteration of this network has not been reported in iRBD. In a few studies, however, these regions were reported to show alterations of structural connectivity [40,41] or neural activity [42] in PD. The rostral part of the supplementary motor area (pre-supplementary motor area) [43] and the parahippocampal gyrus are both anatomically connected with the medial parietal lobe [44]. Indeed, these regions are often coactivated during various tasks [45,46]. Together, our results indicated

that functional integration between the pre-supplementary motor area and the parahippocampal gyrus, which may be mediated by the medial parietal lobe, is a network involved in the pathophysiology of α-synucleinopathy even at its prodromal stage.

The FC between the thalamus and the anterior cingulate cortex was stronger in iRBD. The subnuclei of the thalamus, the anterior nucleus of the thalamus in particular, belong to the limbic system and have reciprocal connections with the anterior cingulate cortex [47,48]. Structural and metabolic alterations of the thalamus and the anterior cingulate cortex have been reported to be responsible for psychiatric symptoms in PD [49–51]. Interestingly, the gray matter volume of these regions was smaller in PD with RBD than in those without [52]. We thus presumed that this FC alteration might reflect the RBD-related symptom on the top of α-synucleinopathy.

4.3. Correlation analysis between functional connectivity and behavioral scores

The present patients with iRBD did not exhibit overt motor symptoms. However, the inter-individual variance of subclinical motor symptoms assessed by the MDS-UPDRS Part III score was correlated with those of the cortico-cortical and sensorimotor-cerebellar FCs. Because these FCs involve motor-related cortices, these findings from the correlation analysis were considered reasonable. Because both FCs were stronger in iRBD than HC, these FC alterations could reflect a compensatory reorganization of motor-related brain networks [5]. Our result suggests that FC analysis has the potential to uncover subclinical motor symptoms in α-synucleinopathy.

The correlation analysis also revealed that the inter-individual variations of sensorimotor-cerebellar and intra-cerebellar FCs correlated with those of the MoCA-J score. MoCA-J is a comprehensive cognitive battery for global cognitive functions. Various brain regions networks were reported to be correlated to the score of MoCA-J in α-synucleinopathies [18,53]. A recent study reported that the sensorimotor network was also related to the MoCA-J score [54]. Our result suggested that the sensorimotor network may also underlie cognitive impairment in iRBD patients.

Our interpretation was that the present FC alteration was more likely related to α-synucleinopathy than sleep disorders because the FCs retrieved by ML were correlated with sub-clinical parkinsonism and cognitive decline, not with RBDSQ-J or ESS. However, we cannot completely exclude the possibility that the altered FCs and cognitive disturbance were also the consequence of sleep disturbance.

4.4. Study limitations

This study had limitations. First, as already discussed, the lack of the formal control data is one of the major limitations of the J-PPMI cohort, which requires an external database for comparison with the healthy population. Ideally, a more strictly controlled group should have been collected, potentially reducing the uncontrolled variance across the groups. For example, a screening procedure for sleep disturbance with RBDSQ-J should have been performed. Note, however, that current ML-based technology requires large datasets, which make it impractical to collect study-specific control data for each study. We retrieved the control data from our own database [7,13], in which the MRIs were previously acquired using the same MRI protocol on the same scanner with that for the iRBD participants. The demographic data such as age and sex differed between the iRBD patients and HCs. To mitigate the confounding effects of the group-wise differences in age and sex on the classification, we used a GLM with covariates of age and sex before conducting the ML-based classification. The classifier had similar performance when we only used the data from participants over 60 years of age; hence, we considered the effects of age difference were minimal. In our opinion, it will be increasingly important to develop a method to take advantage of existing databases in the coming era of study efficiency, sustainability, and ML/artificial intelligence.

Second, the spatial resolution of the present rsfMRI was not fine enough to fully capture the latent network alteration of small brain structure. Indeed, the selected FCs were not correlated with the sleep-related symptoms (RBDSQ-J and ESS scores) of patients with iRBD, despite parasomnia being the only clinically robust symptom of participants with iRBD. This negative finding may be attributed to the limitation of current rsfMRI technology to capture the functional alterations of networks involving small brainstem structures that regulate REM sleep [55,56].

Third, the present study was a single-center, cross-sectional study. Because data of an external validation cohort were not available at the time of analysis, we cannot guarantee the generalization of the classification to other iRBD cohorts. For the same reason, the number of participants was not large enough for developing a fully generalizable ML classifier although this is one of the largest rsfMRI studies in the iRBD literature. A larger sample size will allow us to tune hyperparameters for ML, which may hopefully lead to better performance. To this end, we have started to analyze the longitudinal data from the multiple J-PPMI sites, by taking differences in scanners and protocols into account. Therefore, we hope to overcome the present limitations in the near future.

Finally, many iRBD patients received medications including pramipexole, ramelteon and clonazepam. Administration of dopamine agonists can reduce FC in the sensory-motor network, default mode network, and cerebellar-thalamic-cortical pathway in patients with PD [57] while their effects on FC in prodromal PD or healthy population are not known. The effects of ramelteon or clonazepam on FC are not established, but antiepileptic drugs such as valproate and levetiracetam may reduce regional homogeneity of rsfMRI data, thereby potentially influencing FC [58]. Overall, although the potential influence of medication on FC cannot be completely ruled out, the effects would be minor, considering the number of patients on medication, and the heterogeneity of the medication and their potential effects on FC.

5. Conclusions

We developed an ML-based classifier using rsfMRI-derived FC to discriminate between iRBD patients and HCs. The selected FC values explained the subclinical motor and non-motor symptoms of iRBD patients, which indicated that they carried clinically relevant information. And usefulness of ML-based analysis of FC for evaluating latent brain states in iRBD. Despite its potentials, the present classification technology has not yet reached the point where the method is suitable as a diagnostic tool. Technical development and data accumulation should be continued to make the rsfMRI-based classification of iRBD and α-synucleinopathies relevant to clinical practice.

Ethical approval

Approval was obtained from the NCNP ethics committee (A2014-127). The procedures used in this study adhere to the tenets of the Declaration of Helsinki.

Consent to participate and publish

All participants provided written informed consent for the participation and publication.

Funding

This study was supported in part by the Japan Agency for Medical Research and Development (JP18dm0207070, JP18dm0307003) and the Japan Society for Promotion of Science KAKENHI (19H05726, 19H03536, 23H00414) to TH.

CRediT authorship contribution statement

Toma Matsushima: Formal analysis, Software, Visualization, Writing – original draft. **Kenji Yoshinaga:** Formal analysis, Supervision, Writing – review & editing. **Noritaka Wakasugi:** Data curation, Investigation. **Hiroki Togo:** Data curation, Investigation. **Takashi Hanakawa:** Conceptualization, Funding acquisition, Project administration, Resources, Supervision, Validation, Writing – original draft, Writing – review & editing.

Declaration of competing interest

None of the authors have any conflict of interest associated with this work.

References

[1] Postuma RB, Iranzo A, Hu M, Högl B, Boeve BF, Manni R, et al. Risk and predictors of dementia and parkinsonism in idiopathic REM sleep behaviour disorder: a multicentre study. Brain 2019;142:744–59. https://doi.org/10.1093/brain/awz030.

[2] Berg D, Postuma RB, Adler CH, Bloem BR, Chan P, Dubois B, et al. MDS research criteria for prodromal Parkinson's disease. Mov Disord 2015;30:1600–11. https://doi.org/10.1002/mds.26431.

[3] Heinzel S, Berg D, Gasser T, Chen H, Yao C, Postuma RB, et al. Update of the MDS research criteria for prodromal Parkinson's disease. Mov Disord 2019;34:1464–70. https://doi.org/10.1002/mds.27802.

[4] McCarter SJ, Tippmann-Peikert M, Sandness DJ, Flanagan EP, Kantarci K, Boeve BF, et al. Neuroimaging-evident lesional pathology associated with REM sleep behavior disorder. Sleep Med 2015;16:1502–10. https://doi.org/10.1016/j.sleep.2015.07.018.

[5] Brcina N, Hohenfeld C, Heidbreder A, Mirzazade S, Krahe J, Wojtala J, et al. Increased neural motor activation and functional reorganization in patients with idiopathic rapid eye movement sleep behavior disorder. Parkinsonism Relat Disorders 2021;92:76–82. https://doi.org/10.1016/j.parkreldis.2021.10.019.

[6] Rolinski M, Griffanti L, Piccini P, Roussakis AA, Szewczyk-Krolikowski K, Menke RA, et al. Basal ganglia dysfunction in idiopathic REM sleep behaviour disorder parallels that in early Parkinson's disease. Brain 2016;139:2224–34. https://doi.org/10.1093/brain/aww124.

[7] Wakasugi N, Togo H, Mukai Y, Nishikawa N, Sakamoto T, Murata M, et al. Prefrontal network dysfunctions in rapid eye movement sleep behavior disorder. Parkinsonism Relat Disorders 2021;85:72–7. https://doi.org/10.1016/j.parkreldis.2021.03.005.

[8] Yamada G, Ueki Y, Oishi N, Oguri T, Fukui A, Nakayama M, et al. Nigrostriatal dopaminergic dysfunction and altered functional connectivity in REM sleep behavior disorder with mild motor impairment. Front Neurol 2019;10.

[9] Campabadal A, Segura B, Junque C, Iranzo A. Structural and functional magnetic resonance imaging in isolated REM sleep behavior disorder: a systematic review of studies using neuroimaging software. Sleep Med Rev 2021;59:101495. https://doi.org/10.1016/j.smrv.2021.101495.

[10] Rolls ET, Huang C-C, Lin C-P, Feng J, Joliot M. Automated anatomical labelling atlas 3. Neuroimage 2020;206:116189. https://doi.org/10.1016/j.neuroimage.2019.116189.

[11] Nishikawa N, Murata M, Hatano T, Mukai Y, Saitoh Y, Sakamoto T, et al. Idiopathic rapid eye movement sleep behavior disorder in Japan: an observational study. Parkinsonism Relat Disorders 2022;103:129–35. https://doi.org/10.1016/j.parkreldis.2022.08.011.

[12] Iber C, Ancoli-Israel S, Chesson A, Quan SF, for the American Academy of Sleep Medicine. The AASM manual for the scoring of sleep and associated events: rules, terminology and technical specifications. In: Westchester, illinosis. first ed. American Academy of Sleep Medicine; 2007. 2007.

[13] Togo H, Nakamura T, Wakasugi N, Takahashi Y, Hanakawa T. Interactions across emotional, cognitive and subcortical motor networks underlying freezing of gait. NeuroImage Clin 2023;37:103342. https://doi.org/10.1016/j.nicl.2023.103342.

[14] Folstein MF, Folstein SE, McHugh PR. "Mini-mental state". A practical method for grading the cognitive state of patients for the clinician. J Psychiatr Res 1975;12:189–98. https://doi.org/10.1016/0022-3956(75)90026-6.

[15] Jenkinson M, Beckmann CF, Behrens TEJ, Woolrich MW, Smith SM. FSL. Neuroimage 2012;62:782–90. https://doi.org/10.1016/j.neuroimage.2011.09.015.

[16] Whitfield-Gabrieli S, Nieto-Castanon A. Conn: a functional connectivity toolbox for correlated and anticorrelated brain networks. Brain Connect 2012;2:125–41. https://doi.org/10.1089/brain.2012.0073.

[17] Behzadi Y, Restom K, Liau J, Liu TT. A component based noise correction method (CompCor) for BOLD and perfusion based fMRI. Neuroimage 2007;37:90–101. https://doi.org/10.1016/j.neuroimage.2007.04.042.

[18] Aracil-Bolaños I, Sampedro F, Marín-Lahoz J, Horta-Barba A, Martínez-Horta S, Gónzalez-de-Echávarri JM, et al. Tipping the scales: how clinical assessment shapes the neural correlates of Parkinson's disease mild cognitive impairment. Brain Imaging Behav 2022;16:761–72. https://doi.org/10.1007/s11682-021-00543-3.

[19] Yang Y, Ye C, Sun J, Liang L, Lv H, Gao L, et al. Alteration of brain structural connectivity in progression of Parkinson's disease: a connectome-wide network analysis. NeuroImage Clin 2021;31:102715. https://doi.org/10.1016/j.nicl.2021.102715.

[20] Cochen De Cock V, Dotov D, Lacombe S, Picot MC, Galtier F, Driss V, et al. Classifying idiopathic rapid eye movement sleep behavior disorder, controls, and mild Parkinson's disease using gait parameters. Mov Disord 2022;37:842–6. https://doi.org/10.1002/mds.28894.

[21] Lo C, Arora S, Ben-Shlomo Y, Barber TR, Lawton M, Klein JC, et al. Olfactory testing in Parkinson disease and REM behavior disorder. Neurology 2021;96:e2016. https://doi.org/10.1212/WNL.0000000000011743. LP-e2027.

[22] Berg D, Borghammer P, Fereshtehnejad S-M, Heinzel S, Horsager J, Schaeffer E, et al. Prodromal Parkinson disease subtypes — key to understanding heterogeneity. Nat Rev Neurol 2021;17:349–61. https://doi.org/10.1038/s41582-021-00486-9.

[23] Wing YK, Li SX, Mok V, Lam SP, Tsoh J, Chan A, et al. Prospective outcome of rapid eye movement sleep behaviour disorder: psychiatric disorders as a potential early marker of Parkinson's disease. J Neurol Neurosurg Psychiatry 2012;83:470–2. https://doi.org/10.1136/jnnp-2011-301232.

[24] Iranzo A, Fernández-Arcos A, Tolosa E, Serradell M, Molinuevo JL, Valldeoriola F, et al. Neurodegenerative disorder risk in idiopathic REM sleep behavior disorder: study in 174 patients. PLoS One 2014;9:e89741. https://doi.org/10.1371/journal.pone.0089741.

[25] Postuma RB, Adler CH, Dugger BN, Hentz JG, Shill HA, Driver-Dunckley E, et al. REM sleep behavior disorder and neuropathology in Parkinson's disease. Mov Disord 2015;30:1413–7. https://doi.org/10.1002/mds.26347.

[26] Schenck CH, Boeve BF, Mahowald MW. Delayed emergence of a parkinsonian disorder or dementia in 81% of older men initially diagnosed with idiopathic rapid eye movement sleep behavior disorder: a 16-year update on a previously reported series. Sleep Med 2013;14:744–8. https://doi.org/10.1016/j.sleep.2012.10.009.

[27] Baggio HC, Abos A, Segura B, Campabadal A, Uribe C, Giraldo DM, et al. Cerebellar resting-state functional connectivity in Parkinson's disease and multiple system atrophy: characterization of abnormalities and potential for differential diagnosis at the single-patient level. NeuroImage Clin 2019;22:101720. https://doi.org/10.1016/j.nicl.2019.101720.

[28] Borroni B, Premi E, Formenti A, Turrone R, Alberici A, Cottini E, et al. Structural and functional imaging study in dementia with Lewy bodies and Parkinson's disease dementia. Parkinsonism Relat Disorders 2015;21:1049–55. https://doi.org/10.1016/j.parkreldis.2015.06.013.

[29] Fereshtehnejad S-M, Yao C, Pelletier A, Montplaisir JY, Gagnon J-F, Postuma RB. Evolution of prodromal Parkinson's disease and dementia with Lewy bodies: a prospective study. Brain 2019;142:2051–67. https://doi.org/10.1093/brain/awz111.

[30] Högl B, Stefani A, Videnovic A. Idiopathic REM sleep behaviour disorder and neurodegeneration — an update. Nat Rev Neurol 2018;14:40–55. https://doi.org/10.1038/nrneurol.2017.157.

[31] Haba-Rubio J, Frauscher B, Marques-Vidal P, Toriel J, Tobback N, Andries D, et al. Prevalence and determinants of rapid eye movement sleep behavior disorder in the general population. Sleep 2018;41. https://doi.org/10.1093/sleep/zsx197.

[32] Cicero CE, Giuliano L, Luna J, Zappia M, Preux P-M, Nicoletti A. Prevalence of idiopathic REM behavior disorder: a systematic review and meta-analysis. Sleep 2021;44. https://doi.org/10.1093/sleep/zsaa294.

[33] Ibrahim B, Suppiah S, Ibrahim N, Mohamad M, Hassan HA, Nasser NS, et al. Diagnostic power of resting-state fMRI for detection of network connectivity in Alzheimer's disease and mild cognitive impairment: a systematic review. Hum Brain Mapp 2021;42:2941–68. https://doi.org/10.1002/hbm.25369.

[34] Byun J-I, Kim H-W, Kang H, Cha KS, Sunwoo J-S, Shin J-W, et al. Altered resting-state thalamo-occipital functional connectivity is associated with cognition in isolated rapid eye movement sleep behavior disorder. Sleep Med 2020;69:198–203. https://doi.org/10.1016/j.sleep.2020.01.010.

[35] Campabadal A, Abos A, Segura B, Serradell M, Uribe C, Baggio HC, et al. Disruption of posterior brain functional connectivity and its relation to cognitive impairment in idiopathic REM sleep behavior disorder. NeuroImage Clin 2020;25:102138. https://doi.org/10.1016/j.nicl.2019.102138.

[36] Li G, Chen Z, Zhou L, Yao M, Luo N, Kang W, et al. Abnormal intrinsic brain activity of the putamen is correlated with dopamine deficiency in idiopathic rapid eye movement sleep behavior disorder. Sleep Med 2020;75:73–80. https://doi.org/10.1016/j.sleep.2019.09.015.

[37] Marques A, Roquet D, Matar E, Taylor NL, Pereira B, O'Callaghan C, et al. Limbic hypoconnectivity in idiopathic REM sleep behaviour disorder with impulse control disorders. J Neurol 2021;268:3371–80. https://doi.org/10.1007/s00415-021-10498-6.

[38] Wu T, Hallett M. The cerebellum in Parkinson's disease. Brain 2013;136:696–709. https://doi.org/10.1093/brain/aws360.

[39] Liu J, Shuai G, Fang W, Zhu Y, Chen H, Wang Y, et al. Altered regional homogeneity and connectivity in cerebellum and visual-motor relevant cortex in Parkinson's disease with rapid eye movement sleep behavior disorder. Sleep Med 2021;82:125–33. https://doi.org/10.1016/j.sleep.2021.03.041.

[40] Deng X, Liu Z, Kang Q, Lu L, Zhu Y, Xu R. Cortical structural connectivity alterations and potential pathogenesis in mid-stage sporadic Parkinson's disease. Front Aging Neurosci 2021;13.

[41] Ma L-Y, Chen X-D, He Y, Ma H-Z, Feng T. Disrupted brain network hubs in subtype-specific Parkinson's disease. Eur Neurol 2017;78:200. https://doi.org/10.1159/000477902. –9.

[42] Zhang Y, Wang X, Li Y. Disrupted dynamic pattern of regional neural activity in early-stage cognitively normal Parkinson's disease. Acta Radiol 2021;63:1669–77. https://doi.org/10.1177/02841851211055401.

[43] Geyer S, Luppino G, Rozzi S. Chapter 27 - motor cortex. In: Mai JK, Paxinos G, editors. Hum. Nerv. Syst.. third ed. third ed. San Diego: Academic Press; 2012. p. 1012–35. https://doi.org/10.1016/B978-0-12-374236-0.10027-6.
[44] Johansen-Berg H, Behrens TEJ, Robson MD, Drobnjak I, Rushworth MFS, Brady JM, et al. Changes in connectivity profiles define functionally distinct regions in human medial frontal cortex. Proc Natl Acad Sci USA 2004;101: 13335–40. https://doi.org/10.1073/pnas.0403743101.
[45] Liu D, Chen Q, Shi B, Qiu J. The brain mechanism of mind popping based on resting-state functional connectivity. Neuroreport 2019;30:790–4. https://doi.org/10.1097/WNR.0000000000001286.
[46] Spagna A, Hajhajate D, Liu J, Bartolomeo P. Visual mental imagery engages the left fusiform gyrus, but not the early visual cortex: a meta-analysis of neuroimaging evidence. Neurosci Biobehav Rev 2021;122:201–17. https://doi.org/10.1016/j.neubiorev.2020.12.029.
[47] Mai JK, Forutan F. Chapter 19 - thalamus. In: Mai JK, Paxinos G, editors. Hum. Nerv. Syst.. third ed. third ed. San Diego: Academic Press; 2012. p. 618–77. https://doi.org/10.1016/B978-0-12-374236-0.10019-7.
[48] Morgane PJ, Galler JR, Mokler DJ. A review of systems and networks of the limbic forebrain/limbic midbrain. Prog Neurobiol 2005;75:143–60. https://doi.org/10.1016/j.pneurobio.2005.01.001.
[49] Apostolova I, Lange C, Frings L, Klutmann S, Meyer PT, Buchert R. Nigrostriatal degeneration in the cognitive part of the striatum in Parkinson disease is associated with frontomedial hypometabolism. Clin Nucl Med 2020;45:95–9. https://doi.org/10.1097/RLU.0000000000002869.
[50] Maillet A, Krack P, Lhommée E, Météreau E, Klinger H, Favre E, et al. The prominent role of serotonergic degeneration in apathy, anxiety and depression in de novo Parkinson's disease. Brain 2016;139:2486–502. https://doi.org/10.1093/brain/aww162.
[51] Prange S, Metereau E, Maillet A, Lhommée E, Klinger H, Pelissier P, et al. Early limbic microstructural alterations in apathy and depression in de novo Parkinson's disease. Mov Disord 2019;34:1644–54. https://doi.org/10.1002/mds.27793.
[52] Boucetta S, Salimi A, Dadar M, Jones BE, Collins DL, Dang-Vu TT. Structural brain alterations associated with rapid eye movement sleep behavior disorder in Parkinson's disease. Sci Rep 2016;6:26782. https://doi.org/10.1038/srep26782.
[53] Li M-G, Bian X-B, Zhang J, Wang Z-F, Ma L. Aberrant voxel-based degree centrality in Parkinson's disease patients with mild cognitive impairment. Neurosci Lett 2021;741:135507. https://doi.org/10.1016/j.neulet.2020.135507.
[54] Crockett RA, Hsu CL, Dao E, Tam R, Eng JJ, Handy TC, et al. Painting by lesions: white matter hyperintensities disrupt functional networks and global cognition. Neuroimage 2021;236:118089. https://doi.org/10.1016/j.neuroimage.2021.118089.
[55] Dugger BN, Murray ME, Boeve BF, Parisi JE, Benarroch EE, Ferman TJ, et al. Neuropathological analysis of brainstem cholinergic and catecholaminergic nuclei in relation to rapid eye movement (REM) sleep behaviour disorder. Neuropathol Appl Neurobiol 2012;38:142–52. https://doi.org/10.1111/j.1365-2990.2011.01203.x.
[56] Torontali ZA, Fraigne JJ, Sanghera P, Horner R, Peever J. The sublaterodorsal tegmental nucleus functions to couple brain state and motor activity during REM sleep and wakefulness. Curr Biol 2019;29:3803–3813.e5. https://doi.org/10.1016/j.cub.2019.09.026.
[57] Ballarini T, Růžička F, Bezdicek O, Růžička E, Roth J, Villringer A, et al. Unraveling connectivity changes due to dopaminergic therapy in chronically treated Parkinson's disease patients. Sci Rep 2018;8:14328. https://doi.org/10.1038/s41598-018-31988-0.
[58] Xiao F, Koepp MJ, Zhou D. Pharmaco-fMRI: a tool to predict the response to antiepileptic drugs in epilepsy. Front Neurol 2019;10:1203. https://doi.org/10.3389/fneur.2019.01203.